Hot Deformation Resistance of an AA5083 Alloy under High Strain Rates

SHI-RONG CHEN, CHUNG-YUNG WU, YEN-LIANG YEH and YI-LIANG OU

New Materials Research & Development Department
China Steel Corporation

To produce hot-rolled plates having a superiorly precise dimensional quality, axisymmetric compression tests using the Gleeble 3800 simulator were carried out to assess hot deformation resistance of an AA5083 alloy under high strain rates. Sharp temperature rises and load cell ringing characterized by vibrational load responses were encountered at strain rates higher than 20 s^{-1} while sample buckling occurred at low temperatures. The load cell ringing was corrected using a moving average method with a two-way filtering operation to correct phase distortion. Isothermal flow curves were obtained by fitting the instantaneous temperatures into a binomial function, while the buckling was removed by controlling the sample height. Through the corrections, a hyperbolic sine equation was derived and data of hot tensile test having strain rates lower than 3 s^{-1} were successfully extended to 100 s^{-1}. Effects of temperature, strain rate and work hardening behaviors on the flow curves were quantitatively analyzed accordingly and a new constitutive equation was constructed to predict the hot deformation resistance of the AA5083 alloy for high speed rolling.

Keywords: Axisymmetric compression test, Load cell ringing, Temperature rise, Zener-Hollomon parameter, Hyperbolic sine equation

1. INTRODUCTION

To produce aluminum plates having a superiorly precise dimensional quality, a formula Eq.1, was previously proposed to predict hot deformation resistance of an AA5083 alloy[1], where σ, Th, ε, ε_p and $\dot{\varepsilon}$ are flow stress, homologous temperature being the test temperature T divided by solidus of the alloy (843 K), strain, peak strain 0.14 and strain rate, respectively. The formula followed the basic form of Eq.2 and could faithfully describe the flow behaviors of work hardening at low temperatures as well as work softening at high temperatures. It was derived from friction-free tensile tests using strain rates lower than 3 s^{-1}. Tensile strain as high as 0.7 could be obtained at high temperatures, nevertheless, such high strain data were not available at low temperatures because of limited elongation. Similarly, the elongation decreased with increasing strain rate.

$$\sigma = (-570 + 814 / Th - 195 / Th^2) \times [1.16 \times (\varepsilon/\varepsilon_p)^{-0.45Th + 0.42} - 0.13 \times (\varepsilon / \varepsilon_p)\,] \times (\dot{\varepsilon} / 2)^{0.37Th - 0.19} \quad \cdots\cdots (1)$$

$$\sigma = f(T) \times f(\varepsilon^n) \times f(\dot{\varepsilon}^m) \quad \cdots\cdots (2)$$

In the present work axisymmetric compression tests using the Gleeble 3800 simulator were carried out to extend the experimental strain rate to 100 s^{-1}. With the advent of high speed compression tests, load cell ringing[2], load response appears as a wave form and sharp temperature rises were encountered. In addition, multi-pass compressions using a long sample could be successfully made when the strain rate was relatively low, but buckling occurred at low temperatures when the strain rate was high. Thus, a direct use of the data under high strain rates is difficult.

Correction of load cell ringing was made firstly, temperature rise was normalized using the temperature function of Eq.1, and buckle behaviors were correlated with sample length h, diameter d and Young's modulus E on the basis of Eq.3. Hyperbolic sine function Eq.4, was subsequently used to link the data of the high speed compression tests with those of the hot tensile test because it could be extended over orders magnitude of the strain rate[3]. Here Z is Zener-Hollomon parameter, Q is activation energy for hot deformation, R is the universal gas constant, A and n are numerical constants, respectively.

$$\text{Buckle load limit} = (\pi^3 E d^4 / 256h^2) \quad \cdots\cdots (3)$$

$$Z = \dot{\varepsilon} \times e^{Q/RT} = A[\sinh(\alpha)]^n \quad \cdots\cdots (4)$$

It was hoped that Eq.1 could be appropriately modified and be applied to a hot rolling mill for the production of the superiorly precise dimensional plates running at high speeds.

2. EXPERIMENTAL PROCEDURES

2.1 Sample preparation

Cylinder samples having a diameter of 10 mm and 15 to 21 mm high were cut from a direct chill cast slab, which was 520 mm thick and 1660 mm wide and homogenized at 520°C for 8 h. Major chemical compositions of the slab are listed in Table 1. To minimize variations of microstructure or cast porosities, the cylinder center was located at a constant depth of 70 mm below free surface of the rolling plain. Metallurgical examinations revealed that the average grain size was 160 μm there.

2.2 Compression test using the Gleeble 3800

Tests were carried out according to the procedures suggested by Roebuck et al[4]. Prior to the test, a hole of 1.7 mm diameter and 5 mm deep was drilled into the plane of mid-length to insert a thermocouple, end faces of the cylinder were coated with Ni-paste and cushioned with graphite foils, the sample was then fitted onto the two anvil faces of the simulator. Samples were electrically heated at 2 °C/s to target temperature, soaked there for another 90 s and then compressed with the Hydrawedge system using a constant strain rate mode. Maximum nominal strain rate was 120 s^{-1} and data of load, displacement and temperature were recorded by a maximum acquisition rate 50 kHz.

The sample temperature during the compression stage remained relatively constant and a smooth flow curve could be obtained when the applied strain rate was low. However, the temperature rose sharply and load cell ringing appeared when the strain rate was higher than 20 s^{-1}. Figure 1 shows typical curves of mean pressure and sample temperature rise observed at 350°C using a nominal strain rate 50 s^{-1}.

2.3 Correction of load cell ringing and temperature rise

The ringing signal in Fig.1 was attributed to the

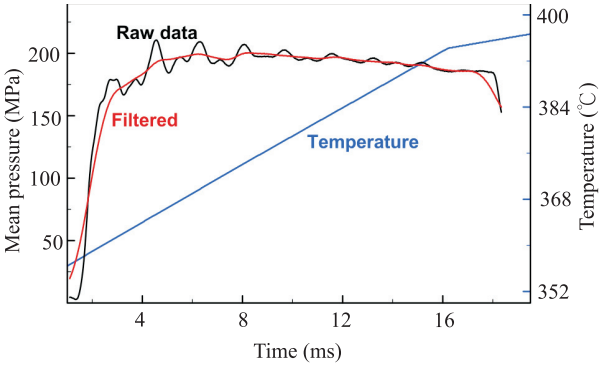

Fig.1. Load cell ringing and temperature rise during a compression test at 350°C using a nominal strain rate 50 s^{-1}.

resonant response of the dynamic system among the testpiece, load cell and Hydrawedge module when subjected to a short duration of excitation. Close examination revealed that the force spectrum bandwidth increased when the strain rate increased beyond 20 s^{-1} providing a wider energy distribution to excite the system resonant response during higher strain rates. The force signal contained a step-like slow-varying signal overlapped with an oscillation component. The latter can be mathematically modeled as an impulse response of a second order system using Eq.5, where symbols A, ζ, ω_n, t, ω_d and φ denote amplitude factor, damping ratio, natural frequency, time, damped natural frequency and phase angle, respectively. The ringing part of the load signal was fitted to Eq.5, substracted from the orignal signal and mean pressure on the sample could be obtained accordingly.

$$f = Ae^{-\zeta\omega_n t}\cos(\omega_d t + \varphi) \quad \cdots\cdots (5)$$

However, this approach involved mode identification and often compounded with inherent nonlinearity of the system stiffness during plastic deformation. Thus, a moving average filter was used to cover all the operating conditions. It was found that the oscillation frequency was around 580 Hz within the scope of the present work. The number of the filter tap was appropriately chosen to assure the cutoff frequency was below that frequency. For a sampling rate of 50 kHz, a 100-tap moving average filter was used. It's -3 dB cutoff frequency was 310 Hz, which was sufficient to smooth out ripple of load signal, as shown in Fig.2. To further correct the delay due to filter operation,

Table 1 Major chemical compositions of the AA5083 alloy

(wt%)

Si	Fe	Cu	Mn	Mg	Cr	Ti	Al
0.11	0.28	0.03	0.69	4.54	0.08	0.014	balance

the load data sequence was filtered in both forward and backward directions to achieve a zero phase distortion.

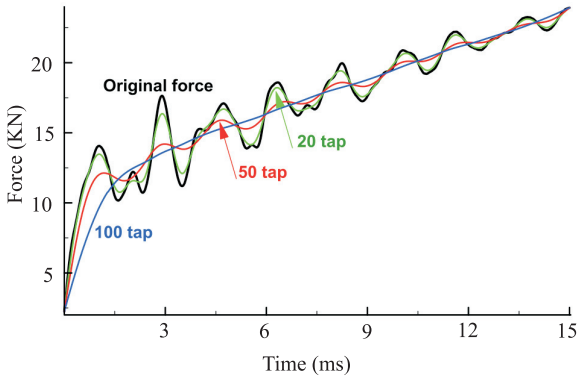

Fig.2. Ringing frequency could be removed by a moving average filter with 100 taps.

After the correction of the load cell ringing, instantaneous temperatures were fitted into the temperature function of Eq.1 and isothermal flow curves were used exclusively. Friction hill of the isothermal flow curves were subsequently corrected using a constant coefficient of friction 0.02 because the degree of sample barreling was minor.

3. RESULTS AND DISCUSSION

3.1 Flow behaviors under high strain rate

Flow stress, as expected, increased with decreasing the temperature. Strain rate dependence of the flow curves tested at 400°C is given in Fig.3, where a corrected curve of strain rate 100 s^{-1} is included. Compared with the work softening curves at low strain rates 0.08 s^{-1} and 0.56 s^{-1}, it is evident that the stress increases with increasing the strain rate as well as the degree of work hardening. Thus, flow curves at strain rates higher than 5.5 s^{-1} were dominated by work hardening i.e., stress increases progressively with increasing the strain within the experimental ranges.

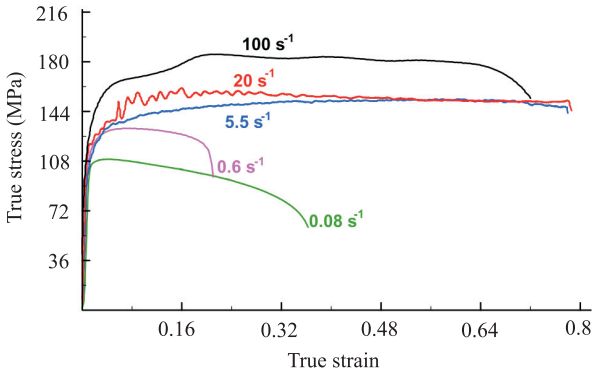

Fig.3. Strain rate dependence of the flow curves tested at 400°C.

Buckling was observed in those samples higher than 18 mm when compressed at temperatures below 350°C using high strain rates. Figure 4 shows the top surface of a 18mm high sample having become oval after being compressed at 330°C using a strain rate 50 s^{-1} because longitudinal axis has been severely tilted. The degree of the buckling was found to increase significantly with decreasing temperature. Abe et al reported that Young's modulus of Al- 5.6 Mg (at%) alloy dropped sharply at temperatures below 350°C [5], but a linear relationship between 200°C and 400°C was proposed by Naimon et al[6]. The present results supported Abe's observation because the Naimon's linear proposal failed to define the critical temperature currently.

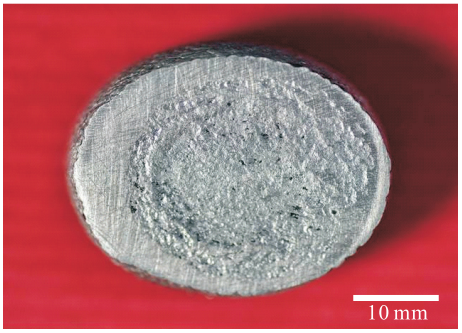

Fig.4. Longitudinal axis buckled when a sample was 18 mm high and compressed at 330°C using a strain rate 50 s^{-1}.

As a result, Abe's data were fitted into Eq.3 and the buckling could be successfully removed by decreasing the sample height. Alternatively, it could also be avoided by decreasing the strain rate but further investigation is required because the effect of strain rate on Young's modulus is currently not clear.

3.2 Hyperbolic sine equation

The stress at a strain of 0.20, $\sigma_{0.2}$, in each curve was intercepted and validated by the hyperbolic sine function Eq.4. Prior to this, the previously measured Q, 173200 J/mol, was used to calculate the Zener-Hollomon parameter Z. This parameter was firstly correlated with the stress and the following exponential function Eq.6 was obtained.

$$Z = 8.57 \times 10^{8} \times \exp(0.082 \times \sigma_{0.2}) \cdots\cdots\cdots\cdots (6)$$

As reported earlier[7,8], α value in Eq.4 can be derived as the ratio of the exponent 0.082 in Eq.6 and n value of power law equation, $Z = A_1 \cdot \sigma_{0.2}^{n}$. However, this equation could not be successfully derived because of high $\sigma_{0.2}$. Thus, a constant α value of 0.015 MPa^{-1}, proposed by Sheppard[9,10], was introduced in the present work.

Figure 5 shows strain rate dependence against the stress, while the stress against temperature is demonstrated in Fig.6. Slope of each curve was obtained by linear regression analyses and averaged as described previously[1,3]. Through a simple multiplication over the mean slope of Figs.5 and 6 and the universal gas constant, the newly derived Q is 174700 J/mol. This value is close to those measured by Sheppard, 171400 J/mol[9,10], Wang[11] and our previous report[1].

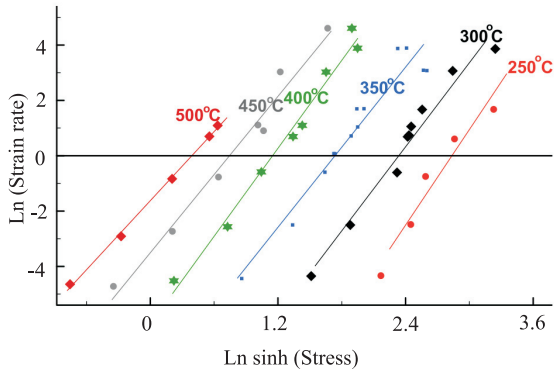

Fig.5. Strain rate dependence against the stress $\sigma_{0.2}$.

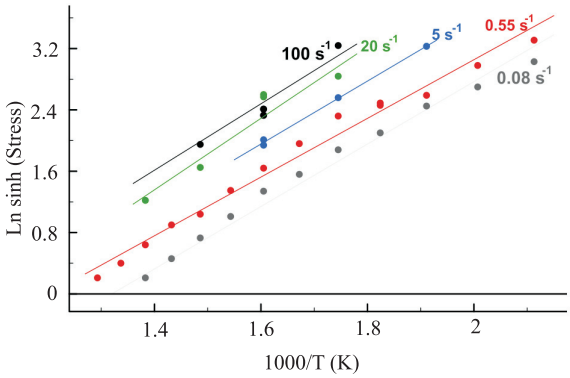

Fig.6. Stress $\sigma_{0.2}$ dependence against the inverse temperature.

The Z parameters of the experimental $\sigma_{0.2}$ were accordingly re-calculated based on the present Q and a new Eq.7 was drawn. The correlation between the Z parameter and the stress $\sigma_{0.2}$ is demonstrated in Fig.7 where the black spots denote hot tensile data and the light spots, the compression data under high strain rates, respectively. It is evident that the data of high strain rates can be correlated with those of hot tensile data having strain rates lower than 3 s^{-1}. The current results support the earlier conclusion that the hyperbolic sine equation can be extended over orders magnitude of the strain rate[3].

$$\mathrm{Ln}\,(\dot{\varepsilon} \times e^{174700/RT}) = 24.98 + 5.23 \times \mathrm{Ln}\sinh(0.015 \times \sigma_{0.2}) \cdots\cdots (7)$$

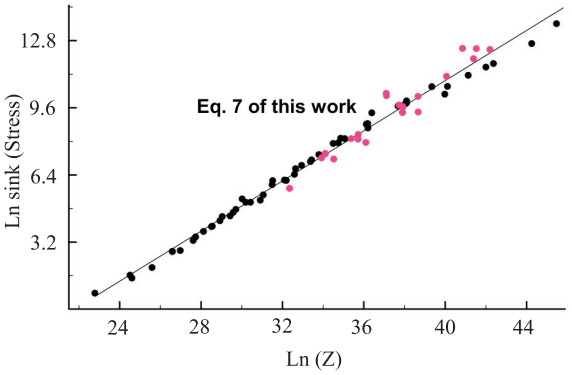

Fig.7. Relationship between stress $\sigma_{0.2}$ and the Zener -Hollomon parameter. (● denote hot tensile data, ● high speed compression data)

3.3 Compound function of strain rate, temperature and work hardening behaviors

Modification of Eq.1 was carried out in a sequence of strain rate sensitivity factor m, followed by the temperature function and then work hardening exponent n. Strain rate sensitivity factor was correlated with homologous temperature Th, as shown in Fig.8. It is clear that the m increased progressively with increasing temperature but its value remained almost unchanged with the introduction of high strain rate compressions. The current observation that m increases with increasing temperature is consistent with earlier reports by Lloyd[12] and Chida et al[13], but contrary to Motomura et al[14] and Kitamura et al[15] who proposed that m was a constant during hot deformation.

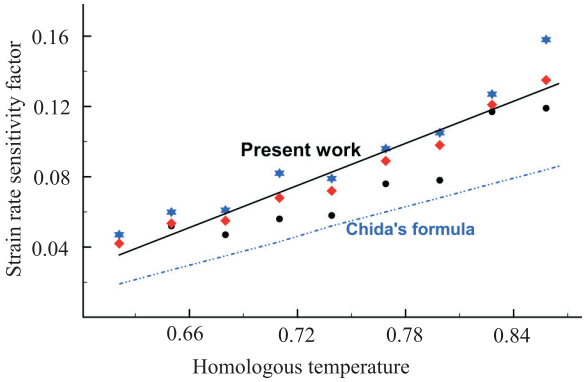

Fig.8. Strain rate sensitivity factor increased with increasing the homologous temperature. (symbols ● ◆ ★ denote strain at 0.10, 0.15 and 0.20, respectively)

A strain rate of 15 s^{-1} was chosen as a standard rate and the following linear equation for the sensitivity factor m was drawn. In Fig.8, the bold line is plotted according to Eq.8, while the dot line denotes Chida's formula. It can be seen that the present m values are higher but the reason is not clear. Additionally, both the

two lines similarly converge at about 185°C i.e., the effect of m is numerically predicted to disappear below this temperature.

$$f(\dot{\varepsilon}^m) = (\dot{\varepsilon}^m / 15)^{0.42Th - 0.23} \quad \cdots\cdots (8)$$

Figure 9 shows all the stress data at strains of 0.10 to 0.65 with an interval of 0.05 within 250 to 450°C. Before the correction using Eq.8, raw data of hot tensile and Gleeble compression fests are denoted by dimond morks. Both the two data scattered largely, but they narrowed down to black spots when Eq.8 was applied. Thereafter, regression analyses of the temperature effect over those black spots revealed that the flow stress could be described by a binomial function Eq.9, as demonstrated by the parabolic line inside Fig.9.

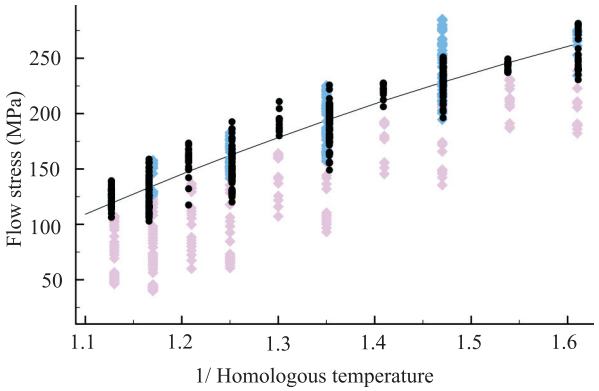

Fig.9. Flow stress increased parabolically with increasing the inverse homologous temperature after being corrected by Eq.8. (● corrected; before correction, ◆ hot tensile test, ◆ high speed compression test)

$$f(T) = -479 + 694 / Th - 145 / Th^2 \quad \cdots\cdots (9)$$

Function to describe the behaviors of both work hardening and work softening was derived in a similar way as reported previously. Since peak strain of the flow curves increases with increasing the strain rate, higher strains were used to minimize discrepancies and the following Eq.10 was obtained. Fig.10 shows that predicted stress-strain curves (solid lines) using Eq.10 for those compressed at 300°C and under various strain rates are close to the observed data (inserted marks) although deviations appeared at lower strains.

Through an additive combination of Eqs.8 to 10, a new formula Eq.11 was consequently derived to predict the hot deformation resistance of the AA5083 alloy.

$$f(\varepsilon^n) = 1.11 \times (\varepsilon / 0.26)^{-0.45Th + 0.42} - 0.06 \times (\varepsilon / 0.26) \quad \cdots\cdots (10)$$

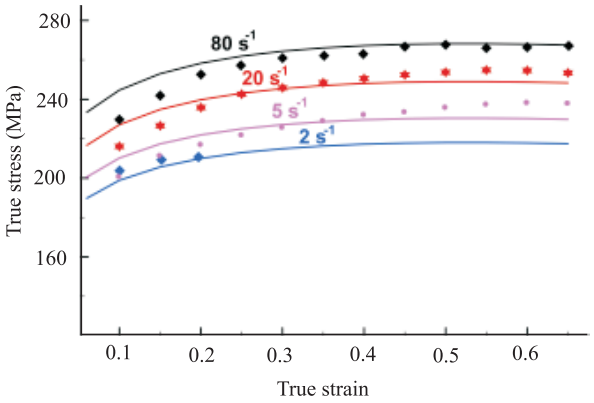

Fig.10. Comparisons of predicted flow curves using Eq. 10 and the measured data (◆★■ ◆) compressed at 300°C.

$$\sigma = (-479 + 694 / Th - 145 / Th^2) \times [1.11 \times (\varepsilon / 0.26)^{-0.45Th + 0.42} - 0.06 \times (\varepsilon / 0.26)] \times (\dot{\varepsilon} / 15)^{0.42Th - 0.23} \quad \cdots\cdots (11)$$

Figure 11 shows a comparison between the present work and the published equations. It can be seen that the experimental data could be well explained by the present equation. In contrast, large deviations of Chida's equation[12] appeared in high stress regions where the temperature has been extended beyond its lower limit (300°C). Deviations were similarly found in Takuda's equation [15] particularly at low stress regions where the flow curves were dominated by work softening.

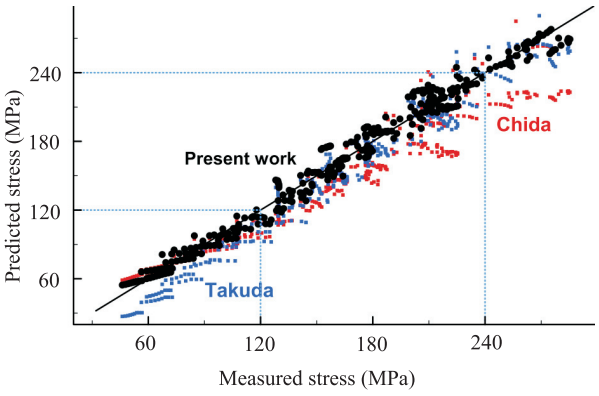

Fig.11. A comparison between the present work and the previously proposed equations. (●present work, ■Chida's Eq., ■Takuda's Eq.)

4. CONCLUSIONS

Hot deformation resistance of the AA5083 alloy under high strain rate compression tested up to 100 s^{-1} has been thoroughly investigated over the respects of

load cell ringing, instantaneous temperature rise, sample buckling and work hardening behaviors. The effects of the temperature T, strain ε and strain rate $\dot{\varepsilon}$ on the flow stress σ have been quantitatively assessed and following conclusions are drawn:

(1) Vibrational force signals during high speed compressions containing a ringing frequency about 580 Hz have been successfully corrected by a moving average filter with 100 taps.

(2) By using the experimentally apparent activation energy for hot deformation 174700 J/mol and an α value 0.015 MPa^{-1}, the flow stress at the strain 0.2 can be described by the following equation:

$$\text{Ln}\,(\dot{\varepsilon} \times e^{174700 / RT}) = 24.98 + 5.23 \times \text{Ln}\,[\sinh(0.015 \times \sigma_{0.2})]$$

(3) Within the experimental ranges of: 250 to 450°C, strains 0.10 to 0.70, and strain rates 0.06 to 100 s^{-1}, flow stress can be described by the equation:

$$\sigma = (-479 + 694 / Th - 145 / Th^2) \times [1.11 \times (\varepsilon / 0.26)^{-0.45Th + 0.42} - 0.06 \times (\varepsilon / 0.26)] \times (\dot{\varepsilon} / 15)^{0.42Th - 0.23}$$

where homologous temperature Th is the test temperature divided by solidus of the alloy (843 K), reference strain and strain rate are 0.26 and 15 s^{-1}, respectively.

REFERENCES

1. Shi-Rong Chen, Yhu-Jen Hwu, Yi-Liang Ou and Yen-Liang Yeh: An Investigation into Hot Deformation Resistance of an AA5083 Alloy, China steel Technical Report, (2012), no. 25, 60-65, also in The First Asian Conference on Aluminum Alloys, Beijing, China, (2013), pp. 244-256.
2. B. Roebuck, M. Brooks and M. G. Gee: Load Cell Ringing in High Rate Compression Tests, (2004), Applied Mechanics and Materials, vol. 1-2, pp. 205-210.
3. W. A. Wong and J. J. Jonas: Aluminum Extrusion as a Thermally Activated Process, Trans. The Metall. Soc. AIME, (1968), vol. 242, pp. 2271- 2280.
4. B. Roebuck, J. D. Lord, M. Brooks, M. S. Loveday, C. M Sellars and R. W. Evans: Measurement of flow stress in hot axisymmetric compression tests, Materials at High Temperature, (2006), 23 (2), pp. 59-83.
5. K. Abe, Y. Tanji, H. Yoshinaga and S. Morozumi: Young's modulus of an Al-Mg alloy at elevated temperatures, J. Japan Institute of Light Metals, (1977), 27 (6), pp. 279-281.
6. E. R. Naimon, H. M. Ledbetter and W. F. Weston: Low-temperature elastic properties of four wrought and annealed aluminum alloys, J. Mater. Sci., (1975), 10, pp. 1309-1316.
7. H. Shi, A. J. Mclaren, C. M. Sellars, R. Shahani and R. Bolingbroke: Constitutive equations for high temperature flow stress of aluminum alloys, Mater. Sci. Tech., (1997), vol. 13, pp. 210-216.
8. C. M. Sellars and W. J. McG. Tegart: Hot Workability, Intern. Metall. Rev., (1972), vol. 17, pp. 1-24.
9. T. Sheppard: Extrusion Processing of Aluminum Alloys, Proceedings 8th Light Metal Congress, (1987), pp. 301-311.
10. H. Yoshida and H. Tanaka: High Temperature Deformation of Aluminum Alloys, Sumitomo Light Metal Technical Reports, (2008), vol. 49, 1, pp. 87-106.
11. Kuo-Hsing Wang: Parameter Analysis and Establishment of Empirical Equations During Hot Rolling Processes of Aluminum Alloy 5182, 2014, Doctorate Dissertation, Department of Mechanical and Electro-Mechanical Engineering National Sun Yat-sen University.
12. D. J. Lloyd: The Deformation of Commercial Aluminum-Magnesium Alloys, Metall. Trans., (1980), 11A, pp. 1287-1294.
13. N. Chida, H. Kimura and Y. Baba: Study on the Flow Stress of Aluminum and Aluminum Alloys at High Temperature, Sumitomo Light Metal Technical Reports, (1980), vol. 19, no. 1-2, p. 3-11.
14. M. Motomura, S. Shimamura and T. Nishimura: On Relating the Resistance to Deformation of Commercial Pure Aluminum and Aluminum Alloy, J. Japan Institute of Light Metals, (1976), vol. 26, no. 9, pp. 432- 440.
15. S. Kitamura and S. Tamiya: Computerization of Hot Rolling for Aluminum Alloys, Kobe Steel Engineering Reports, (1978), vol. 28, no. 2, pp. 94-96.
16. H. Takuda, S. Kikuchi and N. Hatta: Modeling of Comprehensive Formula for Flow Curves of Aluminum Alloys at Elevated Temperatures, J. Japan Society for Technology of Plasticity, (1993), vol. 34, no. 385, pp. 165-170. □